Raman Amplification for Fiber Communications Systems

Jake Bromage, *Member, IEEE, Member, OSA*

Tutorial Paper

***Abstract*—Raman amplification has enabled dramatic increases in the reach and capacity of lightwave systems. This tutorial explains why, starting with the fundamental properties of gain from stimulated Raman scattering. Next, noise accumulation from amplified spontaneous emission is reviewed, and the merits of distributing Raman gain along a transmission fiber are explained. Other sources of noise that are particularly relevant for Raman amplifiers are summarized. Finally, novel Raman pumping schemes that have recently been developed are highlighted.**

***Index Terms*—Distributed amplifiers, optical fiber amplifiers, optical fiber communications, Raman scattering.**

I. Introduction

OPTICAL amplifiers have played a critical role in the telecommunications revolution that began in the early 1990s. For the first time, lightwave communication systems using inline amplifiers could operate over multiple fiber spans without expensive electronic regeneration. Erbium-doped fiber amplifiers (EDFAs) emerged as the technology of choice. The growth of interest in EDFAs, starting around 1990, is clear from Fig. 1, which shows the number of published papers and submitted U.S. patents in this field each year since 1980. The broad-gain bandwidth of EDFAs, extending from 1530 to 1610 nm, is ideal for supporting transmission in the low-loss spectral window of silica-based fiber. In the mid- to late 1990s, commercial systems exploited this broad bandwidth by wavelength-division multiplexing (WDM) tens of signal channels together to achieve capacities of hundreds of gigabits per second.

Research on Raman amplification in optical fibers started early in the 1970s [1]. The benefits from Raman amplification in the transmission fiber were already being investigated in the mid–1980s [2]. However, Raman gain requires more pump power, roughly tens of milliwatts per dB of gain, as compared to the *tenths* of a milliwatt per dB required by EDFAs for small signal powers. This disadvantage, combined with the scarcity of high power pumps at appropriate wavelengths, meant that Raman amplifier research subsided during the commercialization of EDFAs in the early 1990s.

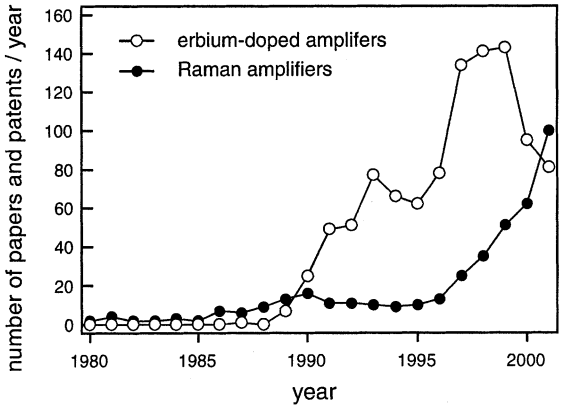

Fig. 1. Number of published papers (conferences and journals of the OSA and IEEE) and submitted U.S. patents each year since 1980 in the fields of EDFAs and Raman amplifiers.

Then, in the mid-1990s, the development of suitable high-power pumps [3] sparked renewed interest (see Fig. 1). Researchers were quick to demonstrate some of the advantages that Raman amplifiers have over EDFAs, particularly when the transmission fiber itself is turned into a Raman amplifier [4], [5]. This, in turn, fueled further advances in Raman pump technology [6]. Fig. 2 shows the exponential increase since 1994 in the capacity-distance product of transmission experiments reported at the postdeadline session of the Optical Fiber Communications conference (OFC). The experiments are categorized by the length of the fiber spans (less than 80 km for submarine-type applications, and greater than or equal to 80 km for terrestrial-type). A number of technologies contributed to these advances: dispersion management, higher modulation rates, fiber engineering, forward-error correction, and advanced modulation formats. Demonstrations that used Raman amplification are circled. The first occurred in 1999, and now Raman amplification is an accepted technique for enhancing system performance.

Since the resurgence of interest in Raman amplification, a number of review articles and chapters have been published [7]–[10]. This paper is based on a tutorial given at OFC 2003 [11]. The goal is to provide a tutorial for those who have some background in fiber optics and lightwave communications, but are new to Raman amplification. (A comprehensive list of references is also provided for readers who wish to pursue any of the topics in more detail.) To this end, the paper is designed to address four main questions: (i) what is Raman amplification?

Manuscript received July 15, 2003.

The author is with OFS Laboratories, OFS, Holmdel, NJ 07733 USA (e-mail: bromage@ofsoptics.com).

Digital Object Identifier 10.1109/JLT.2003.822828

0733-8724/04$20.00 © 2004 IEEE

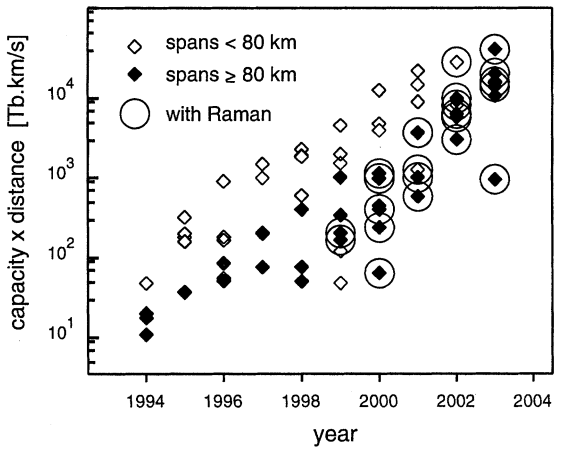

Fig. 2. Capacity-distance products of postdeadline transmission experiments at the Optical Fiber Communications Conference since 1994. Experiments are categorized by the length of their fiber spans. Those using Raman amplification are circled.

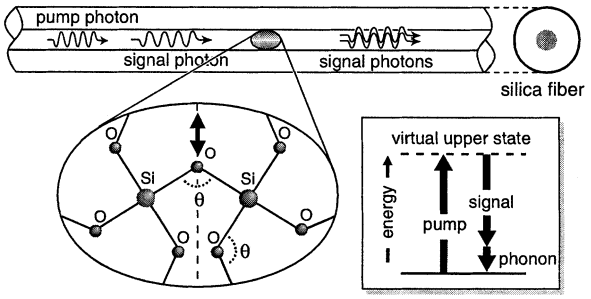

Fig. 3. Schematic depicting amplification by stimulated Raman scattering in an optical silica fiber. The Raman Stokes interaction between a pump and signal photon and the silica molecules converts the pump into a replica of the signal photon, producing an optical phonon.

(ii) where is it used in systems? (iii) why does it improve system performance? and (iv) which noise sources need to be considered?

Section II introduces amplification by stimulated Raman scattering. Section III describes this process in optical fibers from a phenomenological perspective, focusing on properties that are critical to amplifier design and performance. In Section IV, noise from amplified spontaneous emission is reviewed and the enhanced performance that can be obtained with Raman amplifiers is explained. Other sources of noise that are particularly relevant are introduced in Section V. Finally, novel Raman pumping schemes that have recently been developed are highlighted in Section VI.

II. Origin of Raman Scattering

Spontaneous Raman scattering was first discovered by Raman [12], for which he received the Nobel Prize in Physics in 1930. When an optical field is incident on a molecule, the bound electrons oscillate at the optical frequency. This induced oscillating dipole moment produces optical radiation at the same frequency, with a phase shift that leads to the medium's refractive index. Simultaneously, the molecular structure itself is oscillating at the frequencies of various molecular vibrations. Therefore, the induced oscillating dipole moment also contains the sum and difference frequency terms between the optical and vibrational frequencies. These terms give rise to Raman scattered light in the re-radiated field.

In a solid-state quantum mechanical description, optical photons are inelastically scattered by quantized molecular vibrations called optical[1] *phonons* [14]. Photon energy is lost (the molecular lattice is heated) or gained (the lattice is cooled), shifting the frequency of the light. The components of scattered light that are shifted to lower frequencies are called Stokes lines; those shifted to higher frequencies, anti-Stokes lines. The frequency shift is equal to the oscillation frequency of the lattice phonon that is created or annihilated. (The anti-Stokes process is not mentioned further here as it is typically orders of magnitude weaker than the Stokes process in the context of optical communications, making it irrelevant.) Raman scattering can occur in all materials, but in silica glass the dominant Raman lines are due to the bending motion of the Si-O-Si bond (see bond angle θ in Fig. 3).

Raman scattering can also be stimulated by signal light at an appropriate frequency shift from a pump, leading to stimulated Raman scattering (SRS). In this process, pump and signal light are coherently coupled by the Raman process. In a quantum-mechanical description, shown in the energy-level diagram in Fig. 3, a pump photon is converted into a second signal photon that is an exact replica of the first, and the remaining energy produces an optical phonon. The initial signal photon, therefore, has been amplified. This process is considered nonresonant because the upper state is a short-lived virtual state. For a more complete theoretical treatment, the reader is referred to the following: [15]–[18].

III. Raman Amplification in Optical Fibers

A. Properties of Gain From Stimulated Raman Scattering

The following fundamental properties of SRS are critical for designing Raman fiber amplifiers:

1) Raman gain has a spectral shape that depends primarily on the frequency *separation* between a pump and signal, not their absolute frequencies. This follows from energy conservation: their frequency separation must equal the frequency of the optical phonon that is created.
2) Raman gain does not depend on the relative direction of propagation of a pump and signal. The optical branch of the phonon $\omega - k$ diagram is quite flat [14], and so phonons of a given frequency exist with a broad range of momenta or k-vectors. Therefore, momentum conservation is guaranteed irrespective of the relative directions of pump and signal photons.
3) Raman scattering is a fast process (subpicosecond [18]). Because SRS is nonresonant (i.e., the upper state is virtual), there are no long upper-state lifetimes to buffer pump fluctuations as there are, for example, in EDFAs. However, for reasons of efficiency, Raman amplifiers typically consist several kilometers of fiber. Then, a given

[1]Note this is distinct from inelastic scattering caused by acoustic phonons, which is referred to as Brillouin scattering [13].

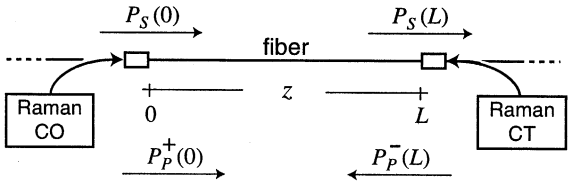

Fig. 4. Schematic of a simple Raman fiber amplifier, that is both copumped (CO) and counterpumped (CT).

portion of signal light can pass through many pump fluctuations if the signal and pump propagate in opposite directions, or if they copropagate at different velocities. This averaging effect can reduce the impact of pump fluctuations (see Section V-E).

4) Raman gain is polarization dependent [19]. The peak coupling strength between a pump and signal is approximately an order of magnitude stronger if they are copolarized than if they are orthogonally polarized (see Section V-D).

B. Amplification of a Signal by a Monochromatic Pump

Fig. 4 shows a schematic of a simple Raman amplifier. It consists of a length L of fiber that is both copumped (CO) and counterpumped (CT) with pump powers P_p^+ and P_p^-, respectively. (Here, and throughout this paper, it is assumed that the signal propagates in the $+z$-direction). Simple ordinary differential equations for describing the amplification of the average signal power (P_s in Watts) are

$$\frac{dP_s}{dz} = -\alpha_s P_s + C_R(\lambda_s,\lambda_p)\left[P_p^+ + P_p^-\right]P_s \quad (1)$$

$$\pm\frac{dP_p^\pm}{dz} = -\alpha_p P_p^\pm - \left(\frac{\lambda_s}{\lambda_p}\right)C_R(\lambda_s,\lambda_p)P_s P_p^\pm \quad (2)$$

where α_s and α_p are the loss coefficients, in units of km^{-1}, at the signal and pump wavelengths, respectively, (λ_s and λ_p). The terms containing a product of the pump and signal powers describe their coupling via SRS. The strength of this coupling is determined by the Raman gain efficiency of the fiber $C_R(\lambda_s,\lambda_p)$, which has units of $(\mathrm{W}\cdot\mathrm{km})^{-1}$.

Fig. 5 shows measurements of C_R for three types of germanosilicate fibers with different 1550-nm effective areas (A_{eff}): a dispersion compensating fiber (DCF, $A_{\mathrm{eff}} = 15\ \mu\mathrm{m}^2$), a nonzero dispersion fiber (NZDF, 55 $\mu\mathrm{m}^2$), and a superlarge effective area fiber (SLA, 105 $\mu\mathrm{m}^2$). For each case the pump wavelength was 1450 nm, and C_R is plotted versus the frequency difference between the pump and signal.[2] The Raman gain efficiency spectra are all roughly triangular in shape, peaking at approximately 13 to 14 THz [20]. These peaks are broader than those of crystalline materials [21], because there a continuum of molecular vibrational frequencies due to the amorphous nature of silica-based glass.

[2]The C_R spectra shown here apply when either the pump or the signal is depolarized, so that the gain is polarization independent. If a polarized pump and signal copropagate with the same polarization state throughout the fiber C_R is approximately a factor of two larger [19].

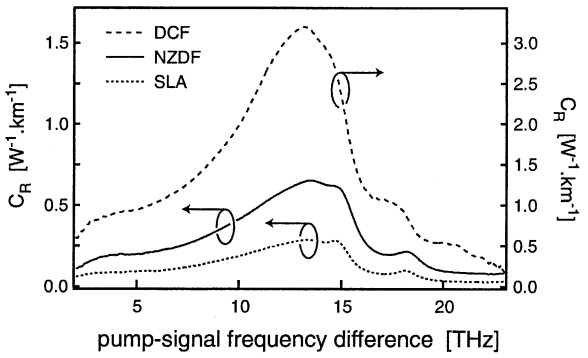

Fig. 5. Raman gain efficiency spectra of three types of germanosilicate fibers, for a pump wavelength of 1450 nm.

There are, however, clear differences between the C_R spectra for these fibers. First of all, their peak values range from 0.29 to 3.2 $(\mathrm{W}\cdot\mathrm{km})^{-1}$. (Note the expanded vertical axis for the DCF spectrum.) These peak values depend on the effective areas and degree of overlap of the pump and signal transverse modes [22], and are *approximately* inversely proportional to the effective area of the signal mode. Differences also result from compositional distinctions between the fibers. Germania ($\mathrm{GeO_2}$), used to increase the refractive index in the fiber core and form the waveguide, also increases the Raman gain efficiency [23]–[26]. Instead of the two peaks seen in the $\mathrm{SiO_2}$ spectra at 13.4 and 14.7 THz, $\mathrm{GeO_2}$ has a single, narrower peak at a slightly lower frequency (13.1 THz). Such differences are clearly visible in the spectra for these fibers because more $\mathrm{GeO_2}$ is used for fibers with small effective areas. Therefore, to predict C_R gain spectra for a given fiber design, one needs a model that takes into account the spatial overlap of the pump and signal transverse modes with the radial compositional profile [27]. In addition, for a given fiber, the maximum value of C_R depends on the specific pump wavelength, typically increasing as the pump wavelength is reduced [28], [29].

The last term in the differential equation for a monochromatic pump [(2)] accounts for depletion of the pump by the signal.[3] For situations where the signal power is small enough ($P_s \ll \alpha_p/C_R$), we can ignore this depletion term. In this case, an analytic solution exists for the *small-signal* net gain of the fiber amplifier:[4]

$$G_{\mathrm{net}} = \frac{P_s(L)}{P_s(0)} = e^{-\alpha_s L}\exp\left(C_R L_{\mathrm{eff}}\left[P_p^+(0) + P_p^-(L)\right]\right). \quad (3)$$

Here L_{eff} is an effective length, within which most of the Raman gain occurs:

$$L_{\mathrm{eff}} = \frac{[1-\exp(-\alpha_p L)]}{\alpha_p}. \quad (4)$$

Often a quantity called the on-off Raman gain is used. This is defined as the increase in signal power at the amplifier output

[3]The factor of (λ_s/λ_p) accounts for the energy difference between the pump and signal photons.

[4]Note that in the definition of optical gain, the output signal power does not include spontaneous Raman scattering generated inside the amplifier.

when the pumps are turned on. Therefore, in the small-signal limit

$$G_{\text{on-off}} = \frac{P_s(L) \text{ with pumps on}}{P_s(L) \text{ with pumps off}} = \exp\left(C_R L_{\text{eff}} \left[P_p^+(0) + P_p^-(L)\right]\right). \quad (5)$$

These equations can be used to estimate how much pump power must be launched into the fiber for a given amount of gain. For example, using 10 km of SLA fiber with signal and pump losses of 0.19 and 0.25 dB/km, respectively, ($\alpha_s = 0.0437$ and $\alpha_p = 0.0576$ km^{-1}), 1.24 W of pump is needed for a small-signal net gain of 10 dB. The higher Raman gain efficiency of DCF means less power is needed (250 mW), even if a shorter length (5 km) and higher signal and pump losses (0.4 and 0.7 dB/km) are assumed. Still, these calculations show that Raman amplification requires pumps that deliver a few hundreds of milliwatts into a single-mode fiber.

Some of the flexibility that Raman amplification offers is clear from Fig. 5. Because SRS does not require a special dopant to provide gain, one can consider using Raman amplification wherever there is fiber in a lightwave system. Broadly speaking, there are two classes of Raman amplifiers. One class is DISTRIBUTED Raman amplifiers, so called because the gain is distributed along the transmission fiber [2], [4]. Another class is called DISCRETE Raman amplifiers because the signal gain occurs within discrete elements in the transmission system. An example of a discrete amplifier is when the DCF inside a dispersion compensating module is Raman-pumped, either to offset the fiber loss [30] or to provide net gain [31].

Raman gain is also flexible in the spectral sense. Because gain depends primarily on the frequency separation between a pump and signal, as long as pump light with the appropriate wavelength and power is available, one can build amplifiers for any band of signal wavelengths. In addition to the C- and L-bands (from 1.53 to 1.61 μm) which are also supported by EDFAs, there have been demonstrations at 1.3 μm [32], 1.4 μm [33], 1.48 μm [34], and 1.65 μm [35].

C. Broad-Band Amplification Using Multiple Pumps

The spectral flexibility of Raman amplification allows the gain spectrum to be shaped by combining multiple pump wavelengths to make a polychromatic pump spectrum. A numerical example of this is shown in Fig. 6. There have been many studies searching for optimization approaches that give the flattest gain with the fewest number of pumps (for example, see [36]). Using this broad-band pumping approach, amplifiers with gain bandwidths greater than 100 nm have been demonstrated [37].

When designing such broad-band Raman amplifiers, one must consider the strong Raman interaction between the pumps [38]. The short wavelength pumps amplify the longer wavelengths, and so more power is typically needed at the shortest wavelengths (see Fig. 6). This interaction between the pumps also affects the noise properties of broad-band amplifiers, which is discussed in Section VI. Differential equations for modeling these phenomena are given in the Appendix.

It is also interesting to note that the asymmetry of the Raman gain efficiency spectrum means that gain at the longest signal

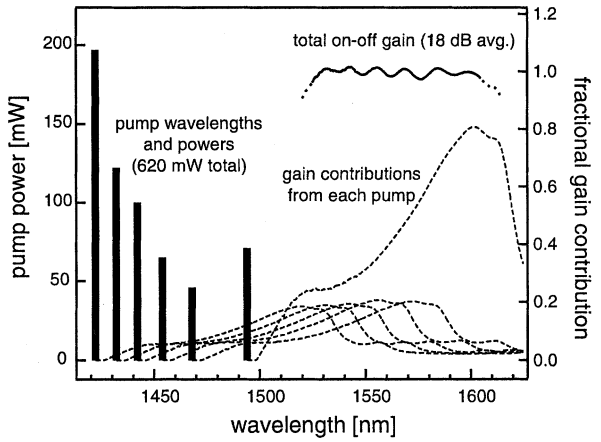

Fig. 6. Numerical example of broad-band Raman gain obtained using a broad pump spectrum to pump a NZDF. Bars show the counterpump wavelengths and input powers. Solid line shows the total small-signal on-off gain. Dashed lines show the fractional gain contribution from each pump wavelength.

wavelengths is determined primarily by the location of the longest wavelength pump(s), even though these pumps are themselves amplified by the shorter wavelength pumps. The shorter wavelength signals, on the other hand, typically receive gain contributions more uniformly from several pumps. This is shown in Fig. 6, where the gain contributions from each pump are shown as dashed lines. All these contributions add to give the total broad-band gain (solid line). Even though only 10% of the total pump power is launched at 1495 nm, it is amplified by the other pumps, leading to 80% of the gain for the longest signal wavelengths.

IV. Noise From Spontaneous Raman Scattering

A. Origin of Spontaneous Raman Scattering

In addition to producing gain, Raman amplifiers produce noise. Understanding how much is produced is crucial because noise accumulation causes transmitted information to be corrupted. The most important source of noise is amplified spontaneous emission (ASE), which is an unavoidable by-product of gain in all optical amplifiers. In the case of Raman amplifiers, ASE is generated by *spontaneous* Raman scattering. The generation and amplification of ASE obeys

$$\pm\frac{dP_A^{\pm}}{dz} = -\alpha_A P_A^{\pm} + C_R(\lambda_A,\lambda_p) P_p P_A^{\pm} + C_R(\lambda_A,\lambda_p)\left[1+\eta(T)\right] h\nu_A B_{\text{ref}} P_p \quad (6)$$

where $P_A^{\pm}$ is the ASE power in one polarization component, in a bandwidth B_{ref}, propagating in the $\pm z$ direction. Here, P_p equals the total depolarized pump power at position z, travelling in both directions.

One difference between this equation and (1) for the signal is the additional inhomogeneous source term in the differential equation. This source term includes a phonon occupancy factor

$$\eta(T) = \frac{1}{\exp\left[\frac{h\Delta\nu}{k_B T}\right] - 1} \quad (7)$$

where h is Planck's constant, k_B is Boltzmann's constant, T is the temperature of the fiber in kelvins, and $\Delta\nu$ is the frequency separation between the pump and signal [14]. At 25 °C, $\eta \approx 0.14$ at the Raman gain peak ($\Delta\nu = 13$ THz), and so it is a small correction factor. If precision is required, however, it needs to be taken into account, particularly for broad-band amplifiers where $\Delta\nu$ can be small when short wavelength channels are close to long-wavelength pumps [39], [40]. Another distinction between the mathematical description of ASE and signals is the boundary conditions, which for ASE are typically $P_A^+(0) = 0$ and $P_A^-(L) = 0$. The general equations for ASE generation with polychromatic pumping and WDM signals are given in the Appendix.

B. Signal-Spontaneous Beat Noise

ASE generation is important because it leads to noise [41]. The dominant type of noise occurs when signal light interferes with copolarized ASE that is propagating in the same direction, producing intensity fluctuations called "signal-spontaneous beat noise." When the signal power is detected by a square-law detector as part of a direct-detection receiver, beat noise frequencies within the detector's electrical bandwidth cause current (or voltage) fluctuations. In a digital system, these fluctuations may lead to errors because signal bits are misinterpreted.

Several quantities can be used to describe the noise properties of Raman amplifiers. One is the optical signal-to-noise ratio (OSNR). This is defined as the ratio of the optical signal power to the power of the ASE in a given reference bandwidth (often 0.1 nm) around the signal wavelength. Usually, the ASE power in all polarizations is included, even though only ASE components with the same polarization state as the signal produce beat noise. Therefore, care needs to be taken when using such a definition if the ASE is partially polarized, as can occur if there is polarization-dependent loss or gain [42]. The OSNR can be measured using a number of techniques, such as ASE interpolation, polarization extinction, and time-domain extinction [43]. Each of these interpolates the amount of ASE actually causing beat noise using ASE at different wavelengths or polarizations from the signal, or using ASE produced at different times.

Another important quantity is the electrical signal-to-noise ratio (SNR). This is the ratio of the signal *electrical* power to the noise power, measured *after photodetection*. Because the electrical signal power is proportional to the photocurrent squared, the SNR is often defined as i^2/σ_i^2, where σ_i^2 is the photocurrent variance. In general, σ_i^2 depends on the magnitude of the optical signal power; that is, on whether a 1 or 0 bit is being detected. Note that the SNR is sensitive not only to signal-spontaneous beat noise, but to any noise mechanism that increases the photocurrent variance. Some of these other noise mechanisms are discussed in Section V. Unlike the OSNR therefore, which is only relevant for noise generated by ASE, the SNR encompasses all sources of intensity noise.

C. Introduction to Noise Figure

An optical amplifier's noise figure (NF) quantifies how much the amplifier degrades a signal's SNR when the signal is amplified. This definition was adapted from the one first used to characterize microwave amplifiers [44].[5] It is defined as

$$\mathrm{NF} = \frac{\mathrm{SNR_{in}}}{\mathrm{SNR_{out}}}. \tag{8}$$

In the case of optical amplifiers it is assumed that the input signal is as noise free as possible and, therefore, is only degraded by shot noise resulting from the fundamental particle nature of light. This assumption ensures that NF has the maximum sensitivity to noise added by the amplifier. Furthermore, it is assumed that $\mathrm{SNR_{out}}$ is measured using an ideal photodetector with a quantum efficiency of 100%.

In the case where signal-spontaneous beat noise is the dominant source of noise added by an optical amplifier, its NF can be approximated in linear units as [43]

$$\begin{aligned}\mathrm{NF} &\approx \frac{2P_A^+(L)}{h\nu B_{\mathrm{ref}} G_{\mathrm{net}}} + \frac{1}{G_{\mathrm{net}}} \\ &= \frac{P_S(0)}{h\nu B_{\mathrm{ref}} \mathrm{OSNR_{out}}} + \frac{1}{G_{\mathrm{net}}}.\end{aligned} \tag{9}$$

The first term corresponds to noise from signal-spontaneous beating and the $1/G_{\mathrm{net}}$ term accounts for shot noise. In general, however, NF can also include contributions from other sources of noise such as spontaneous-spontaneous beating [41] or multiple-path interference (see Section V). Therefore, when designing amplifiers, one must typically consider tradeoffs between minimizing signal-spontaneous beating at the expense of increasing other sources of noise.

If several amplifiers are cascaded together, the total noise figure of the amplifier chain is given by [46]

$$\mathrm{NF_{total}} = \mathrm{NF}_1 + \frac{\mathrm{NF}_2 - 1}{G_1} + \frac{\mathrm{NF}_3 - 1}{G_1 G_2} + \ldots \tag{10}$$

where NF_i and G_i are the noise figure and net gain (in linear units) for the i^{th} amplifier in the chain. This shows that the total noise figure is dominated by the noise figure of the first amplifier (NF_1) if its gain (G_1) is sufficiently high. Hence, many high performance optical (and electrical) amplifiers are multistage amplifiers with a low-noise, high-gain first stage, called a preamplifier stage.

D. Noise Figure of Distributed Raman Amplifiers

The concept of preamplification is crucial for understanding improvements in system performance gained from distributed Raman amplification. As an example, consider a fiber span, 100 km in length, that produces 20 dB of signal loss. Without Raman pumping, a negligible amount of ASE is generated within the fiber span, and so the OSNR is not degraded. Therefore, (9) shows that the NF of the unpumped span equals the second term $(1/G_{\mathrm{net}})$, which in dB equals the 20-dB span loss. If a discrete amplifier follows the span, the total noise figure for the span-plus-amplifier can be calculated using (10), where the first 'amplifier' in the chain is the passive span. Therefore, $\mathrm{NF_{total}}$, in linear units, is the span loss multiplied by the noise figure of

[5]There are many subtleties in defining a noise figure for optical amplifiers. See, for example, [45] and [46] for a more detailed discussion.

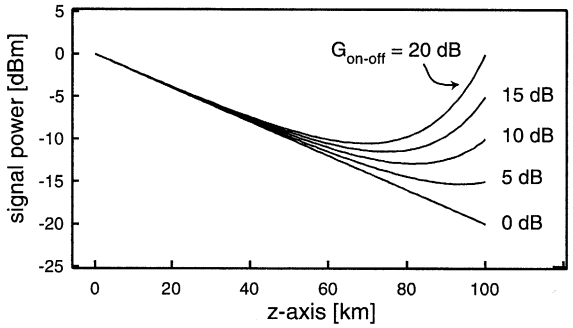

Fig. 7. Simulated signal power evolution for different values of on-off gain.

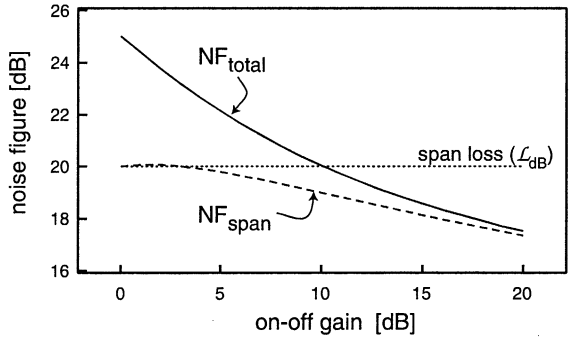

Fig. 8. Simulated values for NF versus on-off Raman gain. The solid line shows the noise figure of a counterpumped fiber span plus discrete amplifier with a 5-dB noise figure. Dashed lines shows the noise figure of the Raman-pumped fiber span alone. Dotted line indicates the loss of the unpumped span.

the discrete amplifier. In dB, if the discrete amplifier NF is 5 dB, $\mathrm{NF_{total}}$ is 25 dB.

Now, if Raman counterpumping is added, the signal power follows trajectories like those shown in Fig. 7. These simulated curves, calculated for on-off gains ranging from 0 dB (pump off) to 20 dB (transparent span), show that Raman pumping effectively converts the last 30 km of fiber into a preamplifier stage. The resulting improvement in $\mathrm{NF_{total}}$ for the span plus discrete amplifier is shown in Fig. 8. Increasing the on-off Raman gain from 0 to 20 dB, reduces the $\mathrm{NF_{total}}$ from 25 to 17.5-dB (solid line). (This improvement is closely related to the increase in the minimum signal power in the span [47], but they are not equal as is sometimes assumed.) In fact, with 20-dB of on-off gain, $\mathrm{NF_{total}}$ is only 0.2-dB higher than the noise figure of the Raman-pumped fiber span, denoted as $\mathrm{NF_{span}}$ (dashed line). This shows that high Raman gain effectively "hides" the noise figure of the discrete amplifier, just as predicted by (10).

E. Effective Noise Figure

This noise figure improvement can be characterized using the concept of an "effective" noise figure[6] (see Fig. 9). This is the noise figure that a fictitious discrete amplifier *would need* when following an unpumped span *to give the same noise performance* as a distributed Raman amplifier. Also, the gain of the effective amplifier must equal the on-off Raman gain, so that it

[6]This concept was first used in [48], where it was called "equivalent" NF. Now, however, the term "effective" NF is more widely accepted.

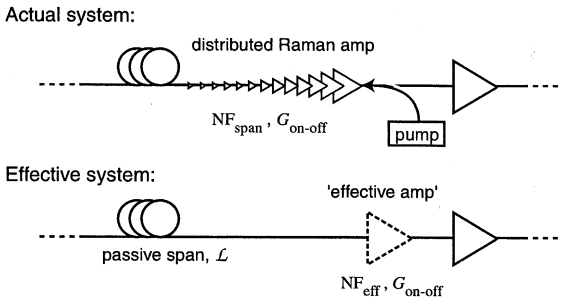

Fig. 9. Actual and "effective" system for Raman counterpumping. Shows the fictitious preamplifier with gain $G_{\mathrm{on-off}}$ and noise figure $\mathrm{NF_{eff}}$ that follows the unpumped span with loss $\mathcal{L}$.

behaves as an equivalent preamplifier to any subsequent amplifiers.

An expression for this effective noise figure $(\mathrm{NF_{eff}})$ can be obtained by equating the noise figures of the two configurations shown in Fig. 9. From (10) it follows that the noise figure of the Raman-pumped fiber span $(\mathrm{NF_{span}})$ must equal

$$\begin{aligned}\mathrm{NF_{span}} &= \mathcal{L} + \frac{\mathrm{NF_{eff}} - 1}{\frac{1}{\mathcal{L}}} \\ &= \mathcal{L} \cdot \mathrm{NF_{eff}} \end{aligned} \tag{11}$$

where $\mathcal{L}$ is the passive span loss and all quantities are in linear units. Therefore, in dB, the noise figure required by the effective amplifier is

$$\mathrm{NF_{eff}(dB)} = \mathrm{NF_{span}} - \mathcal{L}_{\mathrm{dB}}. \tag{12}$$

For the examples shown in Fig. 8, $\mathrm{NF_{span}}$ is less than $\mathcal{L}_{\mathrm{dB}}$ and, therefore, $\mathrm{NF_{eff}}$ is negative in dB. This does not mean that the SNR at the output of a Raman amplifier is higher than at the input, which is not physically possible. In fact, the quantum-limited noise figure for a *high-gain* optical amplifier is 3 dB.[7] Therefore, the fact that a fictitious effective amplifier must have a negative noise figure shows it is impossible for a discrete amplifier to give the same signal-spontaneous beat noise performance as a distributed Raman amplifier.

An effective noise figure is clearly defined and its interpretation straight forward when counterpumping alone is used. However, such an interpretation is not as easy for copumping because gain occurs at the opposite end of the span from the fictitious effective amplifier. Also, if there are many high-power WDM signal channels covering a wide bandwidth, Raman crosstalk between them can cause a significant spectral tilt as power is transferred from the shorter to longer wavelengths [49]. In this case, care needs to be taken to distinguish between the small-signal intrinsic loss of the unpumped fiber span, and the loss when all the channels are launched, which includes Raman-induced spectral tilt.

To understand qualitatively why distributed amplification reduces signal-spontaneous beat noise, compare the two simple configurations shown in Fig. 10. In configuration A, a passive loss element $(\mathcal{L})$ comes before an amplifier (G, NF); in B, the

[7]For example, fully inverted EDFAs with low input coupling losses can have noise figures approaching 3 dB. Amplifiers with *low* gain can have lower noise figures, as can phase-sensitive amplifiers that only amplify one phase quadrature of the signal light [46].

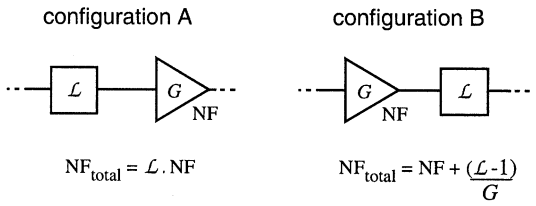

Fig. 10. Two simple configurations A and B where a loss element is placed either before or after an amplifier. Expressions for the total noise figure are shown for each in linear units.

order is reversed. The total noise figures for the composite systems are also shown as $\mathrm{NF_{total}}$ in linear units. Consider a numerical example where $\mathrm{NF} = 3\,\mathrm{dB}$ and $G = \mathcal{L} = 20\,\mathrm{dB}$. Then, configuration A has a total noise figure of 23 dB, whereas the total noise figure of B is only 4.8 dB.

The reason B has a lower $\mathrm{NF_{total}}$ is that the signal and ASE are both attenuated equally by the loss element in this configuration. With A, on the other hand, only the signal is attenuated and so the output OSNR is worse. The key concept here is that the OSNR and, therefore, the noise figure is improved by moving gain before loss. This is exactly what is accomplished when a span is Raman pumped to form a distributed amplifier.

The logical next step is to use copumping to move gain right to the beginning of the fiber span. Indeed, the best $\mathrm{NF_{span}}$ is obtained when only copumping is used, and the span is pumped above transparency. This noise improvement is deceiving, however, because now the maximum signal power in the fiber span has increased significantly. This can increase signal distortions that result from Kerr and other signal nonlinearities [13], counteracting any benefits from reducing noise. These limitations mean the signal launch power must be significantly reduced if large amounts of copumping are added, which in turn reduces the output SNR. Studies have shown that there is an optimum amount of co- and counterpumping that gives the best tradeoff between improving the SNR and reducing signal nonlinear distortions [50]–[53]. The optimal percentage of on-off gain from copumping is between 25% and 50%, depending on system details such as span length and fiber type.

V. Other Sources of Noise in Raman Amplifiers

Here, we introduce some of the other sources of noise that must be taken into account when designing Raman amplifiers.

A. Multiple-Path Interference

Noise from multiple-path interference (MPI) occurs when signal light reaches the receiver by more than one optical path [54]. The simplest example occurs when there are two reflection sites along a system. A small portion of the signal light can be delayed as it is multiply reflected between these sites. Therefore, there are two types of light present at the receiver: the "straight-through" light with average power P_s, and delayed light with power P_{MPI}. Interference between the two converts phase noise (which is otherwise not detected by a square-law receiver) to intensity noise [55], [56].

MPI can be produced in Raman-amplified systems, for example, by discrete reflections at faulty connectors or splices. Raman gain between the reflection sites exacerbates the amount of MPI because the delayed signal is amplified twice when double-passing between each site. Reflection levels in the span, previously considered acceptable without Raman amplification, may, therefore, become intolerable if the reflections lie in regions of high Raman gain [57].

Even if care is taken to eliminate all the discrete reflections within a span, there are still distributed reflections from Rayleigh backscattering in the fiber itself. Rayleigh backscattering occurs when light is elastically reflected by submicron inhomogeneities in a fiber's refractive index that were frozen into the glass when it solidified. MPI results when the signal is backscattered twice, and so this source of MPI is called double-Rayleigh backscattering (DRB). This sets a fundamental limit on the maximum amount of distributed Raman gain that can be used before MPI dominates. This source of MPI also limits gain in discrete Raman amplifiers, which typically use several kilometers of fiber to make efficient use of the pump light. In the case of discrete amplifiers, however, there is more flexibility in the amplifier design, and so techniques such as interstage isolation can be used to frustrate the growth of DRB light [58].

DRB-induced MPI can be simulated using the following equations for the average power of the signal and scattered signal light [54]

$$\frac{dP_s}{dz} = -\alpha_s P_s + C_R P_p P_s \tag{13}$$

$$-\frac{dP_{\mathrm{SRB}}}{dz} = -\alpha_s P_{\mathrm{SRB}} + C_R P_p P_{\mathrm{SRB}} + \kappa P_S \tag{14}$$

$$\frac{dP_{\mathrm{DRB}}}{dz} = -\alpha_s P_{\mathrm{DRB}} + C_R P_p P_{\mathrm{DRB}} + \kappa P_{\mathrm{SRB}} \tag{15}$$

where P_{SRB} is the *single* backscattered power (coupled to P_s, boundary condition at $z = L$), and P_{DRB} is the *double* backscattered power (coupled to P_{SRB}, boundary condition at $z = 0$).

The coupling coefficient κ is approximately equal to $\alpha_R S$, where α_R is the loss per unit length due to Rayleigh scattering, and S is the recapture fraction that determines the fraction of the scattered power captured in the backward propagating mode. Both α_R and S depend on the fiber composition and design [59]–[61]. In particular, S is approximately inversely proportional to A_{eff} at the signal wavelength. Typical values of κ for transmission fibers lie between 0.6 and $1 \times 10^{-4}\mathrm{km}^{-1}$ for fibers with effective areas from approximately 80 to 55 $\mu\mathrm{m}^2$, respectively. Dispersion compensating fibers, on the other hand, can have κ values as high as $5 \times 10^{-4}\mathrm{km}^{-1}$ because they typically have higher concentrations of germanium and smaller effective areas ($\sim 15\ \mu\mathrm{m}^2$).

A separate OSNR, denoted here as $\mathrm{OSNR_{MPI}}$, is often used to characterize the amount of MPI light.[8] This is the ratio of P_s to P_{MPI}, analogous to the OSNR for describing ASE accumulation. One important distinction, however, is that the MPI light typically has a similar optical bandwidth to the signal light, and, therefore, a reference bandwidth is not needed. Care needs to be taken to define the polarization properties of the MPI light because MPI noise is only produced by the component of the

[8]MPI can also be described using a crosstalk ratio (R_C), which is simply the inverse of $\mathrm{OSNR_{MPI}}$ [54]. R_C is predominantly used when describing the performance of a single component, whereas $\mathrm{OSNR_{MPI}}$ is generally favored when considering the cumulative effect of many components or amplifiers in a system.

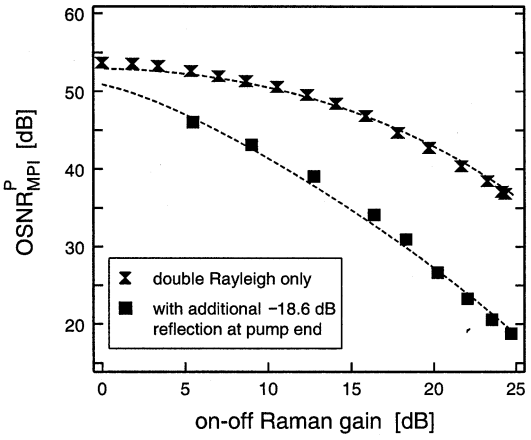

Fig. 11. MPI-OSNR versus on-off Raman gain for simple counterpumped amplifier consisting of 100-km of NZDF. Measurements and simulations are shown for DRB only, or with a reflector added at the pump end of the span [63].

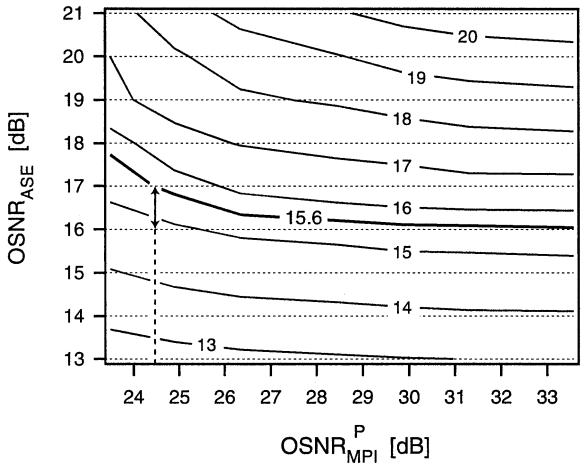

Fig. 12. Contour plot showing the measured Q-factors for 10-Gb/s NRZ data as a function of ASE and MPI OSNRs. Reference [65].

MPI light that is copolarized with the signal $(P^P_{\rm MPI})$. For example, in the case of DRB-induced MPI, moderate birefringence of the fiber causes the DRB-light to be depolarized, and so $P^P_{\rm MPI} \approx (5/9)P_{\rm DRB}$ [62]. To account for this, $\rm OSNR^P_{MPI}$ is used here to describe the ratio of P_S to $P^P_{\rm MPI}$.

Fig. 11 shows $\rm OSNR^P_{MPI}$ values for a simple distributed Raman amplifier [63]. In this case, 100 km of NZDF $(A_{\rm eff} = 55\ \mu{\rm m}^2)$ was counter pumped at 1450 nm, and $\rm OSNR^P_{MPI}$ at 1550 nm was measured using a self-homodyne measurement technique [40], [43]. The markers show the measurement results and the dashed lines show simulation predictions based on (13)–(15). With no Raman pumping, the background level from DRB throughout the fiber span was 54 dB. As the gain was increased, additional DRB was generated and amplified in the high-gain section of the span. This degraded $\rm OSNR^P_{MPI}$ to approximately 36 dB for 25 dB of gain. Also shown in Fig. 11 is the deterioration that occurred when an additional discrete reflector was placed at the pump input to the span. This sent a small fraction of the signal power (1.4%) back into the span, and so now only a single Rayleigh scattering event was required to produce additional MPI power. At on-off gains exceeding 15 dB, this reflector reduced $\rm OSNR^P_{MPI}$ by as much as 20 dB.

If MPI is too large, system performance is degraded, leading to an increase in bit-error ratio (BER) or, equivalently, a decrease in Q-factor [64]. One way to quantify the impact of MPI is to evaluate how much ASE-OSNR improvement is needed to counteract a decrease in $\rm OSNR_{MPI}$ and maintain the same Q-factor. Fig. 12 shows such measurements in the form of contours of constant Q-factor for nonreturn-to-zero (NRZ) data at 10 Gb/s [65]. The axes show the received $\rm OSNR_{ASE}$ and $\rm OSNR^P_{MPI}$, which could be varied independently. At $Q = 15.6$ dB (corresponding to a BER of 10^{-9}), $\rm OSNR^P_{MPI}$ values larger than 30 dB had little impact. However, if $\rm OSNR^P_{MPI}$ was reduced to 24.5 dB, an increase in $\rm OSNR_{ASE}$ of 1 dB was required to maintain the same Q-factor. This value of $\rm OSNR^P_{MPI}$ for such a 1-dB penalty is representative, but the exact value depends on the modulation format [66] and the source of MPI [67].

Another way to characterize DRB-induced MPI in a Raman amplifier is in terms of the amplifier's noise figure. Such analysis should include the spectral differences between MPI, which typically has the same spectrum as the signal, and ASE, which is typically much broader. As a consequence, the relative impact of beat noise from the signal beating with either ASE or MPI light depends on the details of any optical and electrical filtering inside the receiver. If it is assumed that the signal spectra and all filters are Gaussian, an analytic term can be added to (9) to include the contribution from DRB-induced MPI [68]. If the bandwidth of the optical filter is much larger than either the signal bandwidth (B_s) or electrical filter bandwidth (B_e), this term simplifies to give

$$\begin{aligned}\rm NF_{total} &\approx \rm NF_{sig-spon} + \rm NF_{shot} + \rm NF_{DRB} \\ &\approx \frac{2P_A^+(L)}{h\nu B_{\rm ref} G_{\rm net}} + \frac{1}{G_{\rm net}} + \frac{\left(\frac{5}{9}\right) P_{\rm DRB}}{h\nu \sqrt{\frac{B_e^2+B_s^2}{2}} G_{\rm net}}. \quad (16)\end{aligned}$$

This result has been used to calculate the optimum amounts of co- and counterpumping for distributed Raman amplifiers [52]. Here, as a lowest order approximation, signal distortions from Kerr nonlinearities were assumed equal given the same path-averaged signal power.[9] These results show that the optimum amount of Raman gain is lower if DRB-induced MPI is included. Furthermore, a larger fraction of the gain should come from copumping.

The reason why copumping is beneficial can be understood by considering how the DRB light is generated. Moving gain to the front of the span ensures that any DRB light that is amplified by the full Raman gain at both ends must have also double-passed the net loss of fiber in the center. Therefore, less DRB light is produced for the same total amount of gain if copumping is used [69].

B. Pump-Pump Four-Wave Mixing

Another potential source of noise is four-wave mixing (FWM) between the Raman pumps within an amplifier [70]. FWM is an interaction among four photons through the nonlinear response of bound electrons [13]. Photons at one or more frequencies are annihilated (ν_1, ν_2) and new photons at different frequencies are created (ν_3, ν_4). Energy conservation

[9]The validity of this approximation depends on the fiber dispersion and dispersion maps, and is affected by the type of nonlinearity limiting transmission.

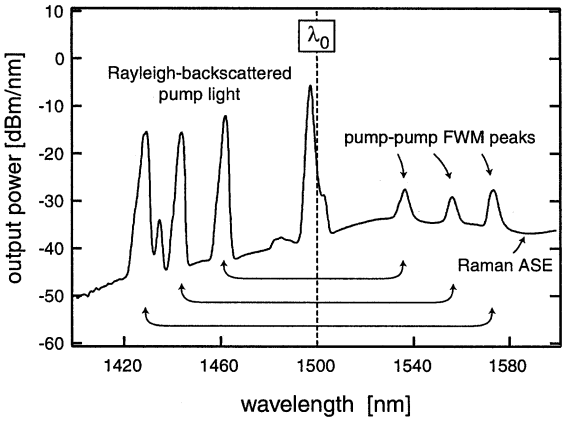

Fig. 13. Output spectrum from a distributed Raman amplifier for the C and L bands, showing pump-pump FWM. (The signals are turned off.) The fiber's zero dispersion wavelength (λ_0) was located close to the 1495-nm pump.

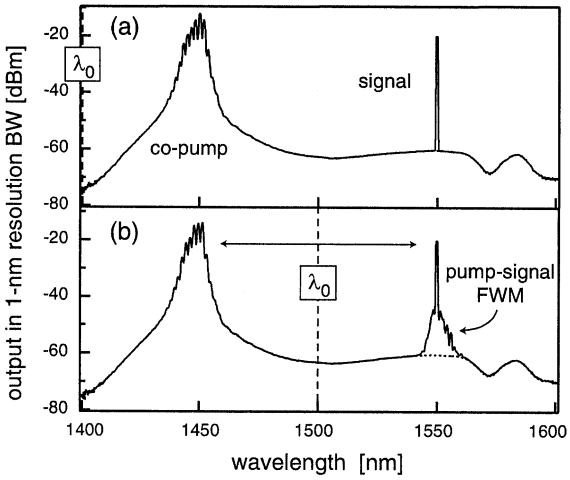

Fig. 14. Example of pump-signal FWM in two amplifiers made from different NZDFs, each providing 3-dB of peak cogain. The output spectra are shown with either the signal on (solid) or off (dotted). FWM is produced close to the signal when λ_0 lies midway between the signal and a copropagating multimode pump [76].

restricts the frequencies at which photons *may* be created such that $\nu_1 + \nu_2 = \nu_3 + \nu_4$. Momentum conservation determines the efficiency of this creation process. This process is most efficient, or "phase matched," when the propagation constants of the four waves (including nonlinear phase terms) obey $\beta_1 + \beta_2 = \beta_3 + \beta_4$. Therefore, the efficiency of FWM depends on the dispersion properties of the fiber [71].

Broad-band Raman amplifiers are pumped using a range of wavelengths (see Fig. 6). Problems arise when FWM between these pumps creates light at new frequencies within the signal band. This new light can interfere with the signal channels, producing beat noise. An example of this is shown in Fig. 13. Here a distributed amplifier covering the C- and L-bands was counter-pumped using four wavelengths to give 20-dB of on-off gain. The figure shows an output spectrum when the signals were turned off.

The peaks below 1500 nm are pump light that was Rayleigh backscattered. The longest wavelength pump (1495 nm) was close to the wavelength at which the fiber had zero dispersion ($\lambda_0 = 1500$ nm). This allowed efficient FWM to occur between two photons from the 1495-nm pump and one photon from any of the other pumps, creating three FWM peaks in the signal band. (As two photons from the same wave are annihilated [$\nu_1 = \nu_2$], this is called *degenerate* FWM.) Even though this light was generated in the same direction as the pump light ($-z$ direction), the process was efficient enough that the Rayleigh backscattered FWM light can be seen above the Raman ASE noise floor. Therefore, the OSNR of any channels in these three regions is significantly degraded.

To overcome this limitation, the fiber dispersion properties must be taken into account when choosing the signal band and pump wavelengths. This process primarily occurs in broad-band amplifiers made from NZDF with a λ_0 located between the pump and signal bands [70], [72], [73].

C. Pump-Signal FWM

Efficient FWM can also occur between pump and signal light if they copropagate in a fiber with a λ_0 located between the pump and signal bands [74]–[76]. Therefore, such pump-signal FWM can be an issue when copumping is used. Here, a signal and pump photon are annihilated, producing a photon at a different pump wavelength and a new FWM photon elsewhere in the signal band.

An example is shown in Fig. 14. Two amplifiers, each made from an NZDF with different dispersion properties, were copumped by a multilongitudinal-mode laser with a center wavelength at 1450 nm to produce 3-dB of on-off gain at 1550 nm. Output spectra are shown for each fiber, taken with the signal either on (solid line) or off (dotted).

In Fig. 14(a), the fiber's λ_0 was 1400 nm. Therefore, poor phase matching ensured that no FWM was produced when the signal was turned on. In Fig. 14(b), however, the λ_0 was 1500 nm, midway between the pump and signal. Here, efficient pump-signal FWM occurred with *both* the pump and signal present, producing additional light at wavelengths close to the signal. This FWM light had a spectrum that closely resembles the mode structure of the pump.

Increasing the pump increased the amount of FWM with a scaling equal to the pump power, P_p, raised to the power of 4.3. This is a stronger pump dependence than the P_p^2-scaling that is predicted by a FWM analysis ignoring Raman gain. Such *Raman-enhanced* pump-signal FWM can severely degrade the OSNRs of WDM channels for certain fiber dispersion conditions if the copump and signal wavelengths are not carefully chosen [76].

D. Polarization-Dependent Gain

The Raman gain spectrum of silica depends on the relative orientation of the pump and signal polarization states. Fig. 15 shows two normalized Raman gain spectra for bulk silica, measured when the pump and signal light were either copolarized or orthogonally polarized. The peak gain when they are copolarized is approximately an order of magnitude larger than when they are orthogonal. Note that this applies not only for linearly polarized light, but also in general for elliptical states of polarization.

Polarization-dependent gain (PDG) in fiber Raman amplifiers can lead to transmission impairments. For example, PDG produces random amplitude fluctuations if the relative polarizations

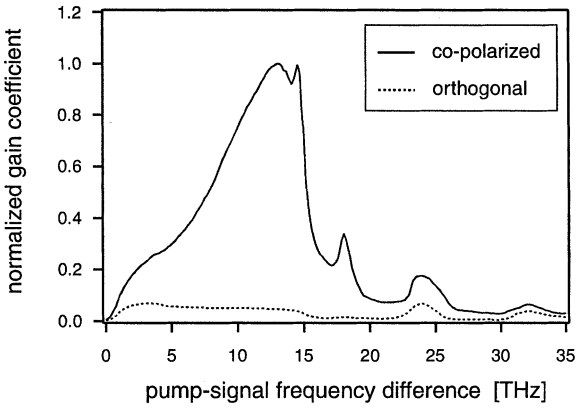

Fig. 15. Raman gain spectra for bulk silica, measured for cases where the pump and signal was either copolarized or orthogonally polarized. Spectra are normalized to the peak of the copolarized spectrum [77].

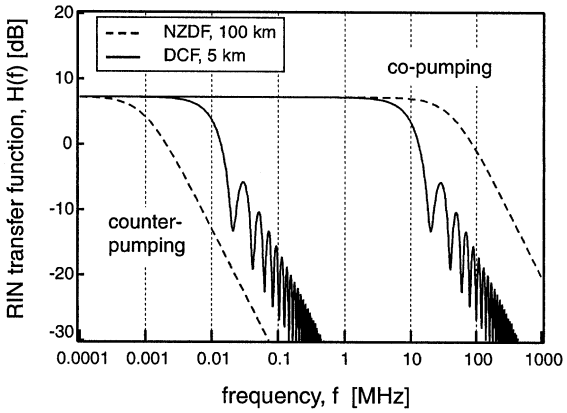

Fig. 16. RIN transfer functions, calculated for 5-km DCF (solid) and 100-km NZDF (dashed) amplifiers. Both co- and counterpumped architectures are shown, with 10-dB on-off gain in all cases. Curves were calculated using the results presented in [84].

of polarized signals and pumps vary randomly. However, the fractional amount of PDG produced in amplifiers consisting of long lengths of fiber is typically not as large as is seen in small bulk samples, thanks to the intrinsic polarization-mode dispersion (PMD) of the fiber [78]. Even when the pump and signal polarization states are aligned at the input, PMD causes their polarizations to evolve differently, changing the strength of the Raman coupling along the fiber [19], [79], [80]. This produces an averaging effect that is even larger if the pumps and signals propagate in opposite directions [81].

Fiber PMD, which itself can directly impair transmission, is not necessary to reduce PDG. Simple measures can be taken to depolarize the pump light, such as polarization-multiplexing the same-wavelength outputs of two independent pumps. Also, single pumps with sufficient spectral bandwidth can be depolarized using fiber Lyot depolarizers formed from a few meters of polarization-maintaining fiber [82], [83]. With such measures, PDG impairments in Raman fiber amplifiers can be eliminated.

E. Noise Transfer From Pumps to Signals

Because stimulated Raman scattering is a nonresonant process, it is inherently fast, occurring over subpicosecond time scales [18]. Therefore, pump power fluctuations can, in principle, be transferred to signals as noise. In fiber amplifiers, however, pumps and signals interact over time scales that are considerably longer because they propagate along many kilometers of fiber. This produces an averaging effect that limits the bandwidth over which pump noise is transferred to the signals.

This phenomenon can be described in the frequency domain as a transfer of relative intensity noise (RIN)[10] from a pump to a signal, using a frequency-dependent transfer function $H(f)$ [84]

$$\mathrm{RIN}_s(f) = H(f)\mathrm{RIN}_p(f). \tag{17}$$

For a given amplifier, $H(f)$ depends on the pumping direction, the pump and signal wavelengths, and the amount of on-off Raman gain. The following properties of the gain fiber are also relevant: its length, pump loss coefficient, dispersion (D), and dispersion slope (D').

Fig. 16 shows calculations of $H(f)$ for two different types of amplifiers, assuming a 1450-nm pump with moderate RIN and a 1550-nm signal. The on-off Raman gain is 10 dB in all cases. The dashed lines correspond to 100-km of NZDF ($\alpha_p = 0.25\,\mathrm{dB/km}$, $D(1550\,\mathrm{nm}) = 4.5\,\mathrm{ps/nm\cdot km}$, $D'(1550\,\mathrm{nm}) = 0.045\,\mathrm{ps/nm^2\cdot km}$). When it is counterpumped, $H(f)$ has a 3-dB corner frequency of ~1-kHz, above which RIN transfer is significantly reduced at a rate of 20 dB per frequency decade. If it is copumped, however, the corner frequency extends out to ~40 MHz, and, therefore, more noise is transferred from the pump.

The co- and counterpumped cases are different because of the amount of averaging that occurs when a given slice of the signal light propagates along the fiber, overlapping with different slices of pump light. In the case of counterpumping, the signal and pump pass through each other, and averaging greatly reduces the impact of pump fluctuations above a few kilohertz. As a rough estimate, significant reductions in RIN transfer occur for any pump fluctuations with a period larger than the propagation time through an effective length ($\sim nL_{\mathrm{eff}}/c$). For copumping however, the pump and signal only pass through each other if there is walk-off caused by chromatic dispersion. Therefore, averaging only reduces RIN transfer at much higher frequencies.

The solid line in Fig. 16 corresponds to a 5-km amplifier made from DCF ($\alpha_p = 0.5\,1\,\mathrm{dB/km}$, $D(1550\,\mathrm{nm}) = -100\,\mathrm{ps/nm\cdot km}$, $D'(1550\,\mathrm{nm}) = 1.0\,\mathrm{ps/nm^2\cdot km}$). The shorter amplifier length produces dips in $H(f)$. The dips occur at pump noise frequencies where an exact integer number of cycles are contained in the gain region, reducing the amount of RIN transfer. Between the dips, the maximum RIN transfer occurs when the number of cycles is an integer plus one-half. If the length of the amplifier is increased, the spacing and amplitude of the dips are reduced until dips are no longer resolvable, as in the 100-km NZDF case. When DCF is copumped, its higher dispersion results in a lower 3-dB corner frequency than that for the NZDF (~10 MHz), despite the shorter interaction length. On the other hand, when the DCF is counterpumped, its shorter length allows for less averaging, and, therefore, the corner frequency is an order of magnitude higher than for the NZDF.

[10]RIN at frequency f is defined as the noise power spectral density at that frequency divided by the square of the average optical power [43].

The amount of Q-factor degradation for a given amplifier design can be estimated using [85]

$$\Delta Q_{\mathrm{dB}} = 10\log_{10}\left(1 + Q_s^2 \int_{f_1}^{f_2} \mathrm{RIN}_s(f)df\right) \qquad (18)$$

where Q_s is a reference Q-factor (in linear units) without RIN transfer, frequencies f_1 and f_2 are the low and high frequency limits of the receiver, and $Q_{\mathrm{dB}} = 20\log_{10}(Q)$. When the noise produced at each amplifier in a chain is uncorrelated and Gaussian, the total accumulated RIN_s is the sum of contributions from each amplifier.

Quieter pumps are needed for copumping because it has a broader RIN transfer bandwidth than counterpumping. As a rough "rule-of-thumb" for a multispan system, copumps with RIN less than -120 dB/Hz are required for negligible Q-penalties, whereas RIN levels as high as -90 dB/Hz are suitable for counterpumped amplifiers. Recently, high-power, narrowband semiconductor pumps, specifically designed for Raman copumping, have been developed with RIN values as low as -145 dB/Hz [86].

F. Pump-Mediated Signal Crosstalk

In copumped amplifiers, fluctuations of the total signal power can degrade the RIN of the copump light if there are significant amounts of depletion. Increased copump RIN can, in turn, add noise to the signals. This process leads to crosstalk between the signals, and, therefore, is a form of cross-gain modulation (XGM). Preliminary simulations and experimental studies have demonstrated this effect [87]–[89], but further work is needed to understand the role of XGM in full WDM transmission systems using copumping.

VI. Novel Raman Pumping Schemes

Some of the novel Raman pumping schemes recently used in transmission experiments are introduced here.

A. Copumping for Broad-Band Amplifiers

In high-capacity broad-band systems, with WDM signal bandwidths exceeding tens of nanometers, stimulated Raman scattering between the signals causes power to be transferred from the shortest to longest wavelength channels. Therefore, the shortest wavelengths experience additional loss. Also, the same interaction between the pumps reduces the penetration depth for the shortest wavelength pumps, further degrading the span noise figure at short signal wavelengths. The longest wavelength pumps, on the other hand, are amplified and so penetrate deeper into the span, as shown in Fig. 17, improving the noise figure for the longest wavelength channels. Moreover, the close spectral proximity of the longest wavelength pumps to the shortest signals increases ASE generation in this spectral region because of its inherent temperature dependence (see Section IV-A). All these effects lead to an OSNR tilt across the signal band with the worst OSNR at shortest wavelengths and the best at longest. Consequently, system performance suffers because system limits are set by the worst channel.

One way to compensate for this tilt is to preferentially copump the shortest wavelength channels [90], [91]. Fig. 18

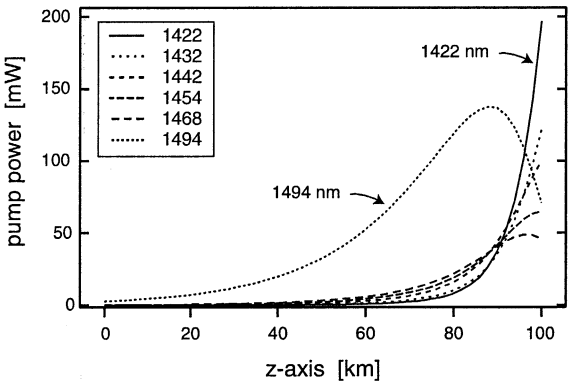

Fig. 17. Simulated pump power evolution for the counterpumped broad-band gain example shown in Fig. 6. Gain for pumps at longer wavelengths is produced at the expense of those at shorter wavelengths.

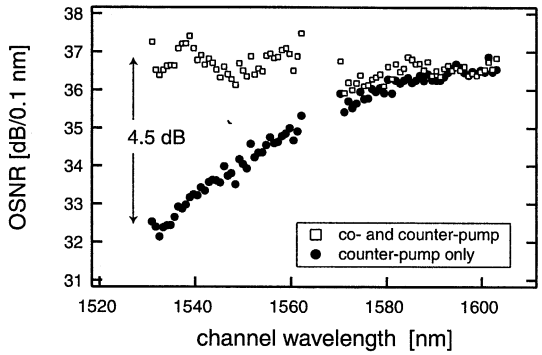

Fig. 18. OSNR tilt correction in C- and L-band system by preferentially copumping the short wavelength channels.

shows measurement results that demonstrate the benefits of this approach. Here 80 channels in the C- and L-band were launched into a 100-km span of NZDF ($A_{\mathrm{eff}} = 55\ \mu\mathrm{m}^2$), with a per-channel launch power of -3 dBm. The square markers show the measured OSNRs when the span was counterpumped to transparency (average $G_{\mathrm{on-off}} = 20$ dB). In this case, four counter pumps were used at 1427, 1447, 1465, and 1495 nm. The resulting OSNR tilt from 1530 to 1610 nm is 4.5 dB.

The circles show the OSNRs when two copumps (1427 and 1447 nm) were added. The cogain they provided was tilted from 7 dB at 1530 nm to 1 dB at 1610. The counterpump powers were reduced to retain the same *total* on-off gain and gain flatness (± 1.2 dB) that was obtained when counterpumping only. These measurements show that OSNR tilt can be eliminated by preferentially copumping the short wavelength channels.

B. Time-Dependent Raman Pumping

Conventional broad-band Raman amplifiers achieve flat gain using a set of pumps at fixed wavelengths with constant output powers. As described above, unwanted interactions between the continuous-wave (CW) pumps can cause impairments such as pump-pump FWM [70] and an OSNR tilt [92]. Recently, new pumping approaches have been developed in which the powers and/or wavelengths of the pumps are intentionally modulated to eliminate these interactions.

In one approach, pumps at fixed wavelengths are time-division multiplexed (TDM) so that only one pump, or a subset of

pumps, are on at any given time [93], [94]. Another approach uses a single pump that is rapidly and repeatedly swept over the necessary wavelength range to achieve broad-band gain [95], [96]. An added benefit of this approach is that significantly lower gain ripple can be achieved because the gain spectrum is not constrained by using a fixed, predetermined number of pump wavelengths [97].

It is important to understand that these approaches are only intended for counterpumping. If used for copumping, the temporal modulation of the pumps would cause severe modulation of the signals. Even when used as counterpumps, the repetition rate of the pump modulation must be fast enough for averaging to eliminate temporal gain variations. If the repetition rate is high enough, the signals see the composite gain from the entire pump spectrum, analogous to a conventional CW-pumped amplifier. As a rule of thumb, a repetition rate greater than 10 kHz is required for temporal gain variations less than 1 dB at an average on-off gain of 15 dB in 100 km of fiber [98].

To date, cost-effective pump technologies have not been developed for these approaches. Therefore, it remains to be seen whether the performance advantages that can be gained by time-dependent Raman pumping are worth the additional cost and complexity.

C. Higher-Order Raman Pumping

Unlike time-dependent Raman pumping, which is designed to eliminate interactions, higher-order pumping *exploits* nnnnninteractions between pumps at different wavelengths. In this scheme, additional pumps are added at wavelengths one or more Stokes shifts below the conventional, first-order pumps [99]. The role of these additional pumps is to amplify the first-order pumps to move the gain for the signals farther from the pump input. In the case of counterpumping, moving gain backward in the span improves the span noise figure. For copumping, moving gain forward in the span allows more signal power to be launched before nonlinear distortions dominate.

A simple numerical example of second-order counterpumping is shown in Fig. 19. In this case 770 mW of pump at 1360 nm was launched along with 20 mW at 1455 nm into 100 km of NZDF ($A_{\text{eff}} = 55\ \mu\text{m}^2$), producing 16 dB of on-off gain at 1550 nm. Fig. 19(a) shows the evolution of the two pumps as they propagate backward into the fiber. The high power 1360-nm pump amplifies the weak 1455-nm seed so that its maximum occurs 13 km into the fiber. Fig. 19(b) shows the resulting small-signal evolution at 1550 nm. Also shown for comparison is the pump power and signal evolution for standard first-order pumping at 1455 nm to the same gain level. Second-order pumping increases the minimum signal power by 1.6 dB above the minimum for first-order pumping, and improves the span noise figure by 1.7 dB.

In this example, the 1360-nm pump power (770 mW) is significantly higher than the power needed for the same gain from conventional first-order pumping at 1455 nm (350 mW). The fact that the process is second-order accounts for 73% of the increase; the higher pump loss (0.35 dB/km instead of 0.25 at 1455 nm) accounts for the remaining 27%. In this case only 20 mW of 1455-nm pump was used to seed the amplifier. Less second-order pump power is required if more first-order seed power is used, but this reduces the noise figure improvement [100].

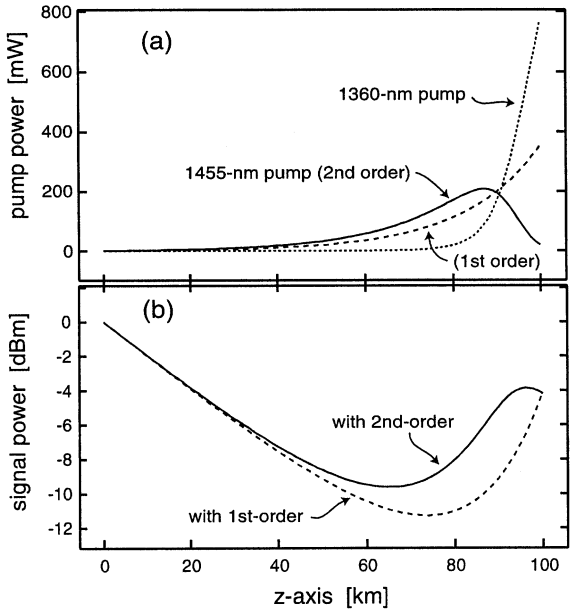

Fig. 19. (a) Simulated evolution of first- and second-order counter pumps. Dashed line shows a first-order pump at 1455 nm that gives the same 16-dB of on-off gain. (b) Corresponding small-signal evolution at 1550 nm.

A number of experiments have shown the benefits of second- or even third-order pumping [101]. One application where second-order pumping is particularly useful is for unrepeatered transmission. Here only one additional pump unit is required, and every dB improvement in span noise figure translates into increased system reach [102]. High pump powers for this application are typically achieved using Raman fiber lasers that can produce watts of depolarized power at any wavelength from 1200 to 1500 nm [100].

VII. Summary

Raman amplification is flexible in the sense that gain can be produced wherever there is optical fiber within a lightwave system. Furthermore, gain can be produced at any wavelength given the appropriate pumps. This flexibility enables system designers to pursue a number of options to get higher system performance at a lower cost.

In this tutorial-based paper, we have discussed the origin of stimulated Raman scattering and outlined the properties of Raman gain that are critical for amplifier design. We have described two types of amplifiers (distributed and discrete) and explained their potential benefits, particularly for reducing noise from ASE accumulation along a transmission system. Also, we have introduced some of the other sources of noise that need to be considered when designing Raman amplifiers. These noise sources influence not only the architecture and gain parameters for a particular amplifier design, but also the choice of components from which it can be built. An understanding of all these issues is necessary to take advantage of Raman amplification to improve system performance and lower costs by increasing a system's reach, data rate, and operating margins.

APPENDIX

The following ordinary differential equations can be used to model broad-band Raman fiber amplifiers using the various quantities described earlier [8], [38]. They are appropriate for polychromatic pump spectra and WDM signals. The average optical power of a pump or signal component at wavelength λ_i, traveling in the positive (negative) z-direction is $P_i^+(P_i^-)$, and obeys

$$\pm\frac{dP_i^{\pm}}{dz} = \left(\gamma_{st,i}^{em} - \gamma_{st,i}^{ab} - \gamma_{sp,i}^{ab} - \alpha_i\right) P_i^{\pm}. \tag{19}$$

Here $\gamma_{st,i}^{em}$ and $\gamma_{st,i}^{ab}$ are stimulated emission and absorption factors, respectively, given by

$$\gamma_{st,i}^{em} = \sum_{\lambda_j<\lambda_i} C_R(\lambda_i,\lambda_j)\left[P_j^+ + P_j^-\right], \quad \text{and}$$
$$\gamma_{st,i}^{ab} = \sum_{\lambda_j>\lambda_i} C_R(\lambda_j,\lambda_i)\left[P_j^+ + P_j^-\right]\left(\frac{\lambda_j}{\lambda_i}\right). \tag{20}$$

where $P_j^{\pm}$ are the average powers of pumps and signals at other wavelengths, λ_j. The factor $\gamma_{sp,i}^{ab}$ accounts for Raman spontaneous absorption, and is given by

$$\gamma_{sp,i}^{ab} = \sum_{\lambda_j>\lambda_i} C_R(\lambda_j,\lambda_i) 2\eta_{ij}(T) h\nu_j B_{\mathrm{ref,j}} \tag{21}$$

and the phonon occupancy factor is

$$\eta_{ij}(T) = \frac{1}{\exp\left(\frac{h[\nu_i-\nu_j]}{k_B T}\right) - 1}. \tag{22}$$

The equation governing the growth of ASE power $P_{A,i}^{\pm}$, in one polarization component and in a bandwidth $B_{\mathrm{ref,i}}$ (in Hz), in either the positive or negative z-directions is

$$\pm\frac{dP_{A,i}^{\pm}}{dz} = \left(\gamma_{st,i}^{em} - \gamma_{st,i}^{ab} - \gamma_{sp,i}^{ab} - \alpha_i\right) P_{A,i}^{\pm}. + \gamma_{sp,i}^{em} \tag{23}$$

where $\gamma_{sp,i}^{em}$ is a spontaneous emission factor, given by

$$\gamma_{sp,i}^{em} = \sum_{\lambda_j<\lambda_i} C_R(\lambda_i,\lambda_j)\left[1+\eta_{ji}(T)\right] h\nu_i B_{\mathrm{ref,i}}. \tag{24}$$

Rayleigh backscattering of pump or ASE light can be included by adding a term $+\kappa P^{\mp}$ to the equations for $P^{\pm}$. Signal backscattering is treated using the approach in Section V-A.

Here it is assumed that the pumps are depolarized. The signals, on the other hand, are typically polarized. This can lead to a numerical error when simulating the Raman interaction between the signals, particularly if their relative polarization states are preserved throughout the fiber amplifier. This error is small, however, when fiber PMD is present. PMD causes the relative polarization states of the signals to evolve, which averages their Raman interaction [19]. Moreover, the largest Raman interaction occurs between signals with the largest frequency separation up to ~100 nm, which are also the signals whose polarization states will diverge in the shortest distance along the fiber.

ACKNOWLEDGMENT

The author would like to acknowledge his many friends and colleagues at OFS, Lucent Technologies, and Furukawa Electric Co. for their collaborations in the design and characterization of optical fibers, amplifiers, and systems. Specifically, he would like to thank J.-C. Bouteiller, M. Du, R.-J. Essiambre, C.-H. Kim, L. E. Nelson, J. W. Nicholson, K. Rottwitt, A. J. Stentz, H. J. Thiele, and P. J. Winzer.

REFERENCES

[1] R. H. Stolen and E. P. Ippen, "Raman gain in glass optical waveguides," *Appl. Phys. Lett.*, vol. 22, pp. 276–278, 1973.
[2] L. F. Mollenauer, J. P. Gordon, and M. N. Islam, "Soliton propagation in long fibers with periodically compensated loss," *IEEE J. Quantum Electron.*, vol. QE-22, pp. 157–173, 1986.
[3] S. G. Grubb, T. Strasser, W. Y. Cheung, W. A. Reed, V. Mizrachi, T. Erdogan, P. J. Lemaire, A. M. Vengsarkar, and D. J. DiGiovanni, "High power, 1.48 μm cascaded Raman laser in germanosilicate fibers," in *Proc. Optical Amplifiers and Their Applicat.*, 1995.
[4] P. B. Hansen, L. Eskildsen, S. G. Grubb, A. J. Stentz, T. A. Strasser, J. Judkins, J. J. DeMarco, R. Pedrazzani, and D. J. DiGiovanni, "Capacity upgrades of transmission systems by Raman amplification," *IEEE Photon. Technol. Lett.*, vol. 9, pp. 262–264, 1997.
[5] T. N. Nielsen, A. J. Stentz, P. B. Hansen, Z. J. Chen, D. S. Vengsarkar, T. A. Strasser, K. Rottwitt, J. H. Park, S. Stulz, S. Cabot, K. S. Feder, P. S. Westbrook, and S. G. Kosinski, "1.6 T b/s (40 × 40 Gb/s) transmission over 4 × 100 km of nonzero-dispersion fiber using hybrid Raman/erbium-doped inline amplifiers," in *Proc. Europ. Conf. Optical Communications*, 1999.
[6] N. Tsukiji, J. Yoshida, T. Kimura, S. Koyanagi, and T. Fukushima, "Recent progress of high power 14XX nm pump lasers," in *Proc. ITcom Active and Passive Optical Components for WDM Communication (Denver)*, 2001, pp. 349–360.
[7] S. Namiki and Y. Emori, "Ultrabroad-band Raman amplifiers pumped and gain equalized by wavelength-division-multiplexed high-power laser diodes," *IEEE J. Select. Topics Quantum Electron.*, vol. 7, pp. 3–16, 2001.
[8] K. Rottwitt and A. J. Stentz, "Raman amplification in lightwave communications systems," in *Optical Fiber Telecommunications, IVA*, I. P. Kaminov and T. Lee, Eds. San Diego, CA: Academic, 2002, pp. 213–257.
[9] M. N. Islam, "Raman amplifiers for telecommunications," *IEEE Select. Topics. Quant. Electron.*, vol. 8, pp. 548–559, 2002.
[10] M. N. Islam, Ed., *Raman Amplifiers for Telecommunications*. New York: Springer-Verlag, 2003.
[11] J. Bromage, "Raman amplification for fiber communication systems," in *Proc. Optical Fiber Communications Conf.*, 2003.
[12] C. V. Raman and K. S. Krishnan, "A new type of secondary radiation," *Nature*, vol. 121, p. 501, 1928.
[13] G. P. Agrawal, *Nonlinear Fiber Optics*, 3rd ed. San Diego, CA: Academic, 2000.
[14] N. W. Ashcroft and N. D. Mermin, *Solid State Physics*. Philadelphia, PA: Saunders College, 1976.
[15] R. W. Hellwarth, "Theory of stimulated Raman scattering," *Phys. Rev.*, vol. 130, pp. 1850–1852, 1963.
[16] A. Penzkofer, A. Laubereau, and W. Kaiser, "High intensity Raman interactions," *Prog. in Quantum Electron.*, vol. 6, pp. 55–140, 1982.
[17] Y. R. Chen and N. Bloembergen, "The stimulated Raman effect," *Amer. J. Phys.*, vol. 35, pp. 989–1023, 1967.
[18] R. H. Stolen, J. P. Gordon, W. J. Tomlinson, and H. A. Haus, "Raman response function of silica-core fibers," *J. Opt. Soc. Amer. B*, vol. 6, pp. 1159–1166, 1989.
[19] R. H. Stolen, "Polarization effects in fiber Raman and Brillouin lasers," *IEEE J. Quantum Electron.*, vol. QE-15, pp. 1157–1160, 1979.
[20] A. R. Chraplyvy, "Optical power limits in multi-channel wavelength-division multiplexed systems due to stimulated Raman scattering," *Electron. Lett.*, vol. 20, pp. 58–59, 1984.
[21] T. T. Basiev, A. A. Sobol, P. G. Zverev, V. V. Osiko, and R. C. Powell, "Comparative spontaneous Raman spectroscopy of crystals for Raman lasers," *Appl. Opt.*, vol. 38, pp. 594–598, 1999.
[22] W. P. Urquhart and P. J. Laybourn, "Effective core area for stimulated Raman scattering in single-mode optical fibers," *Proc. Inst. Elect. Eng.*, vol. 132, pp. 201–204, 1985.

[23] N. Shibata, M. Horigudhi, and T. Edahiro, "Raman spectra of binary high-silica glasses and fibers containing GeO_2, P_2O_5 and B_2O_3," *J. Non-Cryst. Solids*, vol. 45, pp. 115–126, 1981.

[24] S. K. Sharma, D. W. Matson, J. A. Philpotts, and T. L. Roush, "Raman study of the structure of lower pressure chemical vapor deposited and bulk SiO_2-P_2O_5 and SiO_2-GeO_2 glasses," *J. Electrochem. Soc.*, vol. 133, pp. 431–439, 1984.

[25] S. T. Davey, D. L. Williams, B. J. Ainslie, W. J. M. Rothwell, and B. Wakefield, "Optical gain spectrum of GeO_2-SiO_2 Raman fiber amplifiers," *Proc. Inst. Elect. Eng.*, vol. 136, pp. 301–306, 1989.

[26] F. L. Galeener, A. J. Leadbetter, and M. W. Stringfellow, "Comparison of the neutron, Raman, and infrared vibrational spectra of vitreous SiO_2, GeO_2, and BeF_2," *Phys. Rev. B*, vol. 27, pp. 1052–1078, 1983.

[27] J. Bromage, K. Rottwitt, and M. E. Lines, "A method to predict the Raman gain spectra of germanosilicate fibers with arbitrary index profiles," *IEEE Photon. Technol. Lett.*, vol. 14, pp. 24–26, 2002.

[28] K. J. Cordina and C. R. S. Fludger, "Changes in Raman gain coefficient with pump wavelength in modern transmission fibers," in *Proc. Optical Amplifiers and Their Applications*, 2002.

[29] N. Newbury, "Full wavelength dependence of Raman gain in optical fibers: measurements using a single pump laser," in *Proc. Optical Fiber Communications Conf.*, 2003.

[30] Y. Emori, Y. Akasaka, and S. Namiki, "Broadband lossless DCF using Raman amplification pumped by multichannel WDM laser diodes," *Electron. Lett.*, vol. 34, pp. 2145–2146, 1998.

[31] S. A. E. Lewis, F. Koch, S. V. Chernikov, and J. R. Taylor, "Low-noise high gain dispersion compensating broadband Raman amplifier," in *Proc. Optical Fiber Communications Conf.*, 2000.

[32] S. V. Chernikov, Y. Zhu, R. Kashyap, and J. R. Taylor, "High-gain, monolithic, cascaded fiber Raman amplifier operating at 1.3 μm," *Electron. Lett.*, vol. 31, pp. 472–473, 1995.

[33] A. K. Srivastava *et al.*, "Multi-service WDM transmission in 1.3/1.4/1.55 μm bands," in *Proc. Europ. Conf. Optical Communications*, vol. 2, 1999, pp. 200–201.

[34] J. Bromage, J.-C. Bouteiller, H. J. Thiele, K. Brar, J. H. Park, C. Headley, L. E. Nelson, Y. Qian, J. DeMarco, S. Stulz, L. Leng, B. Zhu, and B. J. Eggleton, "S-band all-Raman amplifiers for 40 $\times$ 10 Gb/s transmission over 6 $\times$ 100 km of nonzero dispersion fiber," in *Proc. Optical Fiber Communications Conf.*, 2001.

[35] H. Masuda, S. Kawai, K. Suzuki, and K. Aida, "1.65-μm band fiber Raman amplifier pumped by wavelength-tunable broad-linewidth light source," in *Proc. Europ. Conf. Optical Communications*, 1998, pp. 139–141.

[36] V. E. Perlin and H. G. Winful, "On distributed Raman amplification for ultrabroad-band long-haul WDM systems," *J. Lightwave Technol.*, vol. 20, pp. 409–416, 2002.

[37] Y. Emori, K. Tanaka, and S. Namiki, "100 nm bandwidth flat-gain Raman amplifiers pumped and gain-equalised by 12-wavelength-channel WDM laser diode unit," *Electron. Lett.*, vol. 35, pp. 1355–1356, 1999.

[38] H. Kidorf, K. Rottwitt, M. Nissov, M. Ma, and E. Rabarijaona, "Pump interactions in a 100-nm bandwidth Raman amplifier," *IEEE Photon. Technol. Lett.*, vol. 11, pp. 530–532, 1999.

[39] K. Rottwitt, J. Bromage, M. Du, and A. J. Stentz, "Design of distributed Raman amplifiers," in *Proc. Europ. Conf. Optical Communications*, vol. 2, 2000, pp. 67–71.

[40] C. R. S. Fludger and R. J. Mears, "Electrical measurements of multipath interference in distributed Raman amplifiers," *J. Lightwave Technol.*, vol. 19, pp. 536–545, 2001.

[41] N. A. Olsson, "Lightwave systems with optical amplifiers," *J. Lightwave Technol.*, vol. 7, pp. 1071–1082, 1989.

[42] Y. Sun, I. Lima, A. Lima, H. Jiao, J. Zweck, L. Yan, C. Menyuk, and G. Carter, "Effects of partially polarized noise in a receiver," in *Proc. Optical Fiber Communications Conf.*, 2003.

[43] D. Derickson, Ed., *Fiber Optic Test and Measurement*. Upper Saddle River, NJ: Prentice-Hall, 1998.

[44] H. T. Friis, "Noise figures of radio receivers," in *Proc. IRE*, vol. 32, 1944, pp. 419–422.

[45] H. A. Haus, *Electromagnetic Noise and Quantum Optical Measurements*. Berlin, Germany: Springer-Verlag, 2000.

[46] E. Desurvire, *Erbium-Doped Fiber Amplifiers*. New York: Wiley, 1994, pp. 624–626.

[47] R. G. Smith, "Optical power handling capacity of low loss optical fibers as determined by stimulated Raman and Brillouin scattering," *Appl. Opt.*, vol. 11, pp. 2489–2494, 1972.

[48] P. B. Hansen, L. Eskildsen, A. J. Stentz, T. A. Strasser, J. Judkins, J. J. DeMarco, R. Pedrazzani, and D. J. DiGiovanni, "Rayleigh scattering limitations in distributed Raman pre-amplifiers," *IEEE Photon. Technol. Lett.*, vol. 10, pp. 159–161, 1998.

[49] D. N. Christodoulides and R. B. Jander, "Evolution of stimulated Raman crosstalk in wavelength division multiplexed systems," *IEEE Photon. Technol. Lett.*, vol. 8, pp. 1722–1744, 1996.

[50] P. M. Krummrich, R. E. Neuhauser, H. Bock, W. Fischler, and C. Glingener, "System performance improvements by codirectional Raman pumping of the transmission fiber," in *Proc. Europ. Conf. Optical Communications*, 2001.

[51] A. Carena, V. Curri, and P. Poggiolini, "On the optimization of hybrid Raman/erbium-doped fiber a mplifiers," *IEEE Photon. Technol. Lett.*, vol. 13, pp. 1170–1172, 2001.

[52] R.-J. Essiambre, P. J. Winzer, J. Bromage, and C. H. Kim, "Design of bidirectionally pumped fiber amplifiers generating double Rayleigh backscattering," *IEEE Photon. Technol. Lett.*, vol. 14, pp. 914–916, 2002.

[53] J. Bromage, J.-C. Bouteiller, H. J. Thiele, K. Brar, L. E. Nelson, S. Stulz, C. Headley, J. Kim, A. Klein, G. Baynham, L. V. Jörgensen, L. Grüner-Nielsen, R. L. Lingle Jr., and D. J. DiGiovanni, "High co-directional Raman gain for 200-km spans, enabling 40 $\times$ 10.66 G b/s transmission over 2400 km,," in *Proc. Optical Fiber Communications Conf.*, 2003.

[54] J. Bromage, P. J. Winzer, and R.-J. Essiambre, "Multiple path interference and its impact on system design," in *Raman Amplifiers for Telecommunications*, M. N. Islam, Ed. New York: Springer-Verlag, 2003, ch. 15.

[55] J. A. Armstrong, "Theory of interferometric analysis of laser phase noise," *J. Opt. Soc. Amer.*, vol. 56, pp. 1024–1031, 1966.

[56] J. L. Gimlett and N. K. Cheung, "Effects of phase-to-intensity noise conversion by multiple reflections on gigabit-per-second DFB laser transmission systems," *J. Lightwave Technol.*, vol. 7, pp. 888–895, 1989.

[57] C. H. Kim, J. Bromage, and R. M. Jopson, "Reflection-induced penalty in Raman amplified systems," *IEEE Photon. Technol. Lett.*, vol. 14, pp. 573–575, 2002.

[58] A. J. Stentz, T. Nielsen, S. G. Grubb, T. A. Strasser, and J. R. Pedrazzani, "Raman ring amplifier at 1.3 μm with analog-grade noise performance and an output power of 23 dBm," in *Proc. Optical Fiber Communications Conf.*, 1996.

[59] M. Ohashi, K. Shiraki, and K. Tajima, "Optical loss property of silica-based single-mode fibers," *J. Lightwave Technol.*, vol. 10, pp. 539–543, 1992.

[60] E. Brinkmeyer, "Analysis of the backscattering method for single-mode optical fibers," *J. Opt. Soc. Amer.*, vol. 70, pp. 1010–1012, 1980.

[61] A. H. Hartog and M. P. Gold, "On the theory of backscattering in single-mode optical fibers," *J. Lightwave Technol.*, vol. LT-2, pp. 76–82, 1984.

[62] M. O. van Deventer, "Polarization properties of Rayleigh backscattering in single-mode fibers," *J. Lightwave Technol.*, vol. 11, pp. 1895–1899, 1993.

[63] J. Bromage, C. H. Kim, R. M. Jopson, K. Rottwitt, and A. J. Stentz, "Dependence of double-Rayleigh backscatter noise in Raman amplifiers on gain and pump depletion," in *Proc. Optical Amplifiers and Their Applications*, 2001.

[64] P. J. Winzer, "Optical transmitters, receivers and noise," in *Wiley Encyclopedia of Telecommunications*, J. G. Proakis, Ed: Wiley, 2002, pp. 1824–1840.

[65] J. Bromage, C.-H. Kim, P. J. Winzer, L. E. Nelson, R.-J. Essiambre, and R. M. Jopson, "Relative impact of multiple-path interference and amplified spontaneous emission noise on optical receiver performance," in *Proc. Optical Fiber Communication Conf.*, 2002.

[66] C. Martinelli, G. Charlet, L. Pierre, J. Antona, and D. Bayart, "System inpairment of double-Rayleigh scattering and dependence on modulation format," in *Proc. Optical Fiber Communications Conf.*, 2003.

[67] C. J. Rasmussen, F. Liu, R. J. S. Pedersen, and B. F. Jorgensen, "Theoretical and experimental studies of the influence of the number of crosstalk signals on the penalty caused by incoherent optical crosstalk," in *Proc. Optical Fiber Communications Conf.*, 1999.

[68] P. J. Winzer, R.-J. Essiambre, and J. Bromage, "Combined impact of double-Rayleigh backscatter and amplified spontaneous emission on receiver noise," in *Proc. Optical Fiber Communications Conf.*, 2002.

[69] M. Nissov, K. Rottwitt, H. D. Kidorf, and M. X. Ma, "Rayleigh crosstalk in long cascades of distributed unsaturated Raman amplifiers," *Electron. Lett.*, vol. 35, pp. 997–998, 1999.

[70] R. E. Neuhauser, P. M. Krummrich, H. Bock, and C. Glingener, "Impact of nonlinear pump interactions on broadband distributed Raman amplification," in *Proc. Optical Fiber Communications Conf.*, 2001.

[71] N. Shibata, R. P. Braun, and R. G. Waarts, "Phase-mismatch dependence of efficiency of wave generation through four-wave mixing in single-mode optical fiber," *IEEE J. Quantum Electron.*, vol. QE-23, pp. 1205–1210, 1987.
[72] L. Leng, B. Zhu, S. Stulz, L. E. Nelson, J. C. Bouteiller, P. Kristensen, and L. Grüner-Nielsen, "Experimental investigation of the impact of NZDF zero-dispersion wavelength on broadband transmission in Raman-enhanced systems," in *Optical Fiber Communications Conf.*, 2003.
[73] J.-C. Bouteiller, L. Leng, and C. Headley, "Pump-pump four-wave mixing in distributed Raman amplified systems," *J. Lightwave Technol.*, Mar. 2003.
[74] K. Inoue, "Tunable and selective wavelength conversion using fiber four-wave mixing with two pump lights," *IEEE Photon. Technol. Lett.*, vol. 6, pp. 1451–1453, 1994.
[75] M.-C. Ho, C.-J. Chen, W. S. Wong, and H. K. Lee, "Parametric interactions between pumps and signals in a co-pumped Raman amplifier," in *Proc. Conf. Lasers and Electro-Optics*, 2002.
[76] J. Bromage, P. J. Winzer, L. E. Nelson, and C. J. McKinstrie, "Raman-enhanced pump-signal four-wave mixing in bidirectionally-pumped Raman amplifiers," in *Proc. Optical Amplifiers and Their Applications*, 2002.
[77] From private correspondence with R. H. Stolen.
[78] H. Kogelnik, L. E. Nelson, and R. M. Jopson, "Polarization-mode dispersion," in *Optical Fiber Telecommunications, Vol IVB*, I. Kaminow and T. Li, Eds. New York: Elsevier Science, 2002, pp. 725–862.
[79] Q. Lin and G. Agrawal, "PMD effects in fiber-based Raman amplifiers," in *Optical Fiber Communications Conf.*, 2003.
[80] E. Son, J. Lee, and Y. Chung, "Gain variation of Raman amplifier in birefringent fiber," in *Optical Fiber Communications Conf.*, 2003.
[81] H. H. Kee, C. R. S. Fludger, and V. Handerek, "Statistical properties of polarization dependent gain in fiber Raman amplifiers," in *Proc. Optical Fiber Communications Conf.*, 2002.
[82] K. Böhm, K. Petermann, and E. Weidel, "Performance of Lyot depolarizers with birefringent single-mode fibers," *J. Lightwave Technol.*, vol. LT-1, pp. 71–74, 1983.
[83] J. S. Wang, J. R. Costelloe, and R. H. Stolen, "Reduction of the degree of polarization of a laser diode with a fiber Lyot depolarizer," *IEEE Photon. Technol. Lett.*, vol. 11, pp. 1449–1451, 1999.
[84] C. R. S. Fludger, V. Handerek, and R. J. Mears, "Pump to signal RIN transfer in Raman fiber amplifiers," *J. Lightwave Technol.*, vol. 19, pp. 1140–1148, 2001.
[85] ——, "Pump to signal RIN transfer in Raman fiber amplifiers," *IEEE J. Lightwave Technol.*, vol. 19, pp. 1140–1148, 2001.
[86] Y. Ohki, N. Hayamizu, H. Shimizu, S. Irino, J. Yoshida, N. Tsukiji, and S. Namiki, "Increase of relative intensity noise after fiber transmission in co-propagating Raman pump lasers," in *Proc. Optical Amplifiers and Their Applications*, 2002.
[87] W. Jiang and P. Ye, "Crosstalk in fiber Raman amplification for WDM systems," *IEEE J. Lightwave Technol.*, vol. 7, pp. 1407–1411, 1989.
[88] F. Forghieri, R. W. Tkach, and A. R. Chraplyvy, "Bandwidth of cross talk in raman amplifiers," in *Proc. Optical Fiber Communications Conf.*, 1994.
[89] M. Du, T. N. Nielsen, K. Rottwitt, and A. J. Stentz, "WDM Optical Communication System Using Co-Propagating Raman Amplification,", Tech. Rep. 6 417 958, 2002.
[90] S. Kado, Y. Emori, S. Namiki, N. Tsukiji, J. Yoshida, and T. Kimura, "Broadband flat-noise Raman amplifier using low-noise bi-directionally pumping sources," in *Proc. Europ. Conf. Optical Communications*, 2001.
[91] B. Zhu, L. Leng, L. E. Nelson, L. Grüner-Nielsen, Y. Qian, J. Bromage, S. Stulz, S. Kado, Y. Emori, S. Namiki, P. Gaarde, A. Judy, B. Palsdottir, and R. L. Lingle Jr., "3.2 Tb/s (80 × 42.7 Gb/s) transmission over 20 × 100 km of nonzero dispersion fiber with simultaneous C + L-band dispersioncompensation," in *Proc. Optical Fiber Communications Conf.*, 2002.
[92] C. R. S. Fludger, V. Handerek, and R. J. Mears, "Fundamental noise limits in broadband Raman amplifiers," in *Proc. Optical Fiber Communications Conf.*, 2001.
[93] C. R. S. Fludger, V. Handerek, N. Jolley, and R. J. Mears, "Novel ultrabroadband high performance distributed Raman amplifier employing pump modulation," in *Proc. Optical Fiber Communications Conf.*, 2002.
[94] P. J. Winzer, K. Sherman, and M. Zirngibl, "Experimental demonstration of time division multiplexed Raman pumping," in *Proc. Optical Fiber Communications Conf.*, 2002.
[95] L. F. Mollenauer, A. R. Grant, and P. V. Mamyshev, "Time-division multiplexing of pump wavelengths to achieve ultrabroadband, flat, backward-pumped Raman gain," *Opt. Lett.*, vol. 27, pp. 592–594, 2002.
[96] J. W. Nicholson, J. Fini, J.-C. Bouteiller, J. Bromage, and K. Brar, "A swept-wavelength Raman pump with 69 MHz repetition rate," in *Proc. Optical Fiber Communications Conf.*, 2003.
[97] A. R. Grant, "Calculating the Raman pump distribution to achieve minimum gain ripple," *IEEE J. Quantum Electron.*, vol. 38, pp. 1503–1509, 2002.
[98] P. J. Winzer, J. Bromage, R. T. Kane, P. A. Sammer, and C. Headley, "Tuning speed requirements for time-division multiplexed Raman pump amplifiers," in *Proc. Europ. Conf. Optical Communications*, 2002.
[99] K. Rottwitt, A. J. Stentz, T. N. Nielsen, P. B. Hansen, K. Feder, and K. Walker, "80-km bi-directionally pumped distributed Raman amplifier using second-order pumping," in *Proc. Europ. Conf. Optical Communications*, 1999.
[100] J. C. Bouteiller, K. Brar, J. Bromage, S. Radic, and C. Headley, "Dual-order Raman pump," *IEEE Photon Technol. Lett.*, vol. 15, pp. 212–214, 2003.
[101] S. B. Papernyi, V. I. Karpov, and W. R. L. Clements, "Third-order cascaded Raman amplification," in *Proc. Optical Fiber Communications Conf.*, 2002.
[102] L. Labrunie, F. Boubal, E. Brandon, L. Buet, N. Darbois, D. Dufournet, V. Harvard, P. Le Roux, M. Mesic, L. Piriou, A. Tran, and J.-P. Blondel, "1.6 Terabits/s (160 × 10.66 G bit/s) unrepeatered transmissio nover 321 km using second-order pumping distributed Raman amplification," in *Proc. Optical Amplifiers and Their Applications*, 2001.

Jake Bromage (M'01) was born in London, U.K., in 1967. He received the B.Sc. degree (1st class honors) in physics from the University of St. Andrews, Scotland, in 1991, and the Ph.D. degree in optics from the University of Rochester, NY, in 1999. His thesis "Creating Rydberg electron wavepackets using terahertz pulses," included research into ultrafast lasers and quantum optics.

After graduation he joined Bell Laboratories as a Member of Technical Staff. Currently, he is with the System Testing Group, OFS Labs (formally OFS, Lucent Technologies), Holmdel, NJ. His work includes various aspects of Raman-amplified system design and characterization. He has authored and coauthored more than 30 papers in this field, including a textbook chapter and two tutorials. Currently, he is also a short–course instructor with the Optical Fiber Communications Conference.

Dr. Bromage is a Member of the Optical Society of America (OSA).